Microstructure and load bearing capacity of TiN/NbN superlattice coatings deposited on medical grade CoCrMo Alloy by HIPIMS

HOVSEPIAN, Papken <http://orcid.org/0000-0002-1047-0407>, ARUNACHALAM SUGUMARAN, Arunprabhu <http://orcid.org/0000-0002-5087-4297>, RAINFORTH, Mark, QI, Jiahui, KHAN, Imran and EHIASARIAN, Arutiun

journal of the mechanical behavior of biomedical materials 132 (2022) 105267

Contents lists available at ScienceDirect

Journal of the Mechanical Behavior of Biomedical Materials

journal homepage: www.elsevier.com/locate/jmbbm

Microstructure and load bearing capacity of TiN/NbN superlattice coatings deposited on medical grade CoCrMo alloy by HIPIMS

Papken Ehiasar Hovsepian [a,*], Arunprabhu Arunachalam Sugumaran [a], Mark Rainforth [b], Jiahui Qi [b], Imran Khan [c], Arutiun Papken Ehiasarian [a]

[a] National HIPIMS Technology Centre, Materials and Engineering Research Institute, Sheffield Hallam University, United Kingdom
[b] University of Sheffield, Mappin Street, Sheffield, United Kingdom
[c] Zimmer-Biomet UK Limited, Dorcan Industrial Estate, Swindon, United Kingdom

ARTICLE INFO

Keywords:
Medical implants
Superlattice coating
High power impulse magnetron sputtering
Toughness
Crack initiation

ABSTRACT

In recent years significant progress has been made in the application of various ceramic, namely Metal nitride (MeN) functional coatings to engineer the surfaces of medical implants utilising metal-on-metal (MoM) articulation. This article reports on the load bearing capacity and structural response of TiN/NbN superlattice coatings deposited on medical grade CoCrMo alloy substrate under the application of localised load and the subsequent crack formation mechanism. The coatings have been deposited by mixed High Power Impulse Magnetron Sputtering-Unbalanced Magnetron Sputtering (HIPIMS-UBM) process. In the case of TiN/NbN coating deposited on CoCrMo substrate where $E_{coating}/E_{substrate}$ is as high as 1.81 indicating that the substrate does not provide the necessary load bearing support for the brittle thin film, the utilisation of the Berkovich indentation technique proved to be a potent approach to study coating material as well as structural response to applied concentrated load. FIB/SEM analyses of the indented coatings revealed that in the hard-on-soft material systems cracks will initiate due to sub-coating substrate deformation and then propagate towards the coating surface. The FIB/SEM and low magnification XTEM analysis showed that an exceptionally strong TiN/NbN coating substrate adhesion bonding was achieved due to the utilisation of the HIPIMS pre-treatment. High resolution XTEM analyses revealed, for the first time, that during the indentation a collective rotation and alignment of the individual layers of the superlattice stack takes place without compromising coatings integrity which is clear evidence for the exeptionally high coating fracture toughness. The high toughness of the superlattice structured TiN/NbN coatings combined with their exceptionally high adhesion on madical grade CoCrMo ranks them as a strong candidate for medical implant applications.

1. Introduction

A credible approach to enhance the durability and therefore the lifetime of medical implants is to engineer the load bearing surfaces by the application of functional coating. The demand here is for coating materials with high wear and corrosion resistance, biocompatibility as well as reliable barrier properties to prevent metal ions leaching from the base implant material. This is particularly exacerbated with CoCrMo implant alloys where the release of mechanical wear debris and ions of toxic cancerogenic Cr and Co elements due to tribo-corrosion act synergistically to patient health deterioration (Okazaki and Gotoh, 2005; Wapner, 1991; McGregor et al., 2000). It is therefore of paramount importance that the coating design process follows a strict path of proper material selection, coating structure and architecture selection and finally selection of the coating deposition technology.

Among the metallic materials which possess the necessary high biocompatibility and electrochemical stability are Ta, Nb, Ti, Cr, Zr. Carbon and Me-doped carbon materials are another class of materials, which satisfy these requirements, but clearly the choice is rather limited. Still hard wear resistant coatings such as Ta, TiN, TiNbN and DLC have been successfully developed and widely used in many orthopaedic applications (Blunt et al., 2009; Serro et al., 2009; Yang et al., 2000; Hoseini et al., 2008).

Coating crystallographic structure (amorphous or crystalline), microstructure (granular, columnar or nanocomposite) and architecture (monolithically grown or multilayer with its variations including the

* Corresponding author.
E-mail address: p.hovsepian@shu.ac.uk (P.E. Hovsepian).

https://doi.org/10.1016/j.jmbbm.2022.105267
Received 25 March 2022; Received in revised form 3 May 2022; Accepted 5 May 2022
Available online 10 May 2022

nanoscale multilayer/superlattice architecture) define the mechanical, tribological and barrier properties of the coatings. Here the indisputably winning approach is the utilisation of nanoscale multilayer/superlattice architecture, which allows significant enhancement of the mechanical properties such as achieving superhardness and exceptionally high toughness. Importantly the nanolaminated structure enhances the coating's wear resistance by changing the wear mechanisms (layer by layer on nanoscale) improves the barrier properties such as corrosion resistance due to the presence of a high number of interfaces between the individual layers which hinder inward and outward material transport and densifies the coating due to the specific coating growth mechanism (Hovsepian et al., 2000; Hovsepian et al., 2006; Hovsepian and M ü nz, 2002; Chen et al., 2021). Recently, the National HIPIMS Technology Centre in the UK reported on a novel CrN/NbN coatings developed for joint replacement achieving exceptionally high mechanical performance parameters due to the application of the superlattice structure concept. In biological environments, cytotoxicity, genotoxicity and sensitisation tests carried out *in vitro* the new coatings showed no adverse effects (Hovsepian et al., 2016; Blunn et al., 2019).

Coating deposition technology strongly influences coating load and *in vivo* human environment interactions hence defines coating final performance. The various coating fabrication technologies used to enhance the surface durability of artificial joints such as physical vapor deposition (PVD), chemical vapor deposition (CVD), laser PVD, implantation and electroplating produce coatings with different integrity, surface morphology and very importantly adhesion strength. It has been reported that the synergy between pinhole corrosion and poor adhesion leading to complete coating failure is probably one of the most severe problems encountered in the real-life medical implant applications (Ł apaj et al., 2016). Therefore, the applied technology must be considered based on its ability to produce highly dense, free of growth and surface defects coatings and very importantly allow for coating substrate interface engineering. It is important to mention that the surface pre-treatment (cleaning/etching) prior to the coating deposition which is an integral part of the production process must also be considered very seriously as this has direct implications on the coating adhesion and growth mechanism. To the large family of PVD technologies such as Cathodic arc (CA) evaporation, Magnetron sputtering (MS), Arc Bond Sputtering (ABS) which in principle can be used for treating medical implants in recent years a novel pulse power magnetron sputtering technique, known as HIPIMS was added. The technology was pioneered and upscaled at Sheffield Hallam University, UK by Prof. A. P. Ehiasarian (Ehiasarian and Wei, 2007). The key advantages of the new technology are the production of highly dense and very smooth coatings with exceptionally high adhesion. The availability of highly ionised metal plasma in the discharge influences positively not only the coating structure but importantly allows to engineer the coating substrate interface by implanting metal ions during the pre-treatment stage, which produces strong metallurgical coating substrate bonding and promotes local epitaxial growth of the coating (Ehiasarian et al., 2006, 2007).

Considering the above guidelines, TiN/NbN coating utilising nanoscale multilayer/superlattice structure was deposited by High Power Impulse Magnetron Sputtering technology to protect medical grade CoCrMo alloys for medical implant applications. The tribological, corrosion and barrier properties against metal ion leaching in Hank's solution of this coating were described in detail elsewhere (Sugumaran et al., 2021). However, the coating's fine microstructure on nanoscale and their load bearing capacity and the response of the nanolayered stack of ceramic TiN and NbN under localised load and the subsequent crack formation mechanism due to such load have not been reported. The current paper aims to describe these phenomena which are directly linked to the coating life time in the demanding application to protect medical implants.

2. Materials and methods

2.1. Coating deposition technology

The material combination in TiN/NbN was chosen on the basis of metals, which show the highest biocompatibility and electrochemical stability in the human body. To produce the nanoscale multilayer/superlattice structured coating a computer controlled, industrial size four cathode, HTC 1000-4 coating system, (Hauzer Techno Coating B.V., The Netherlands) enabled with HIPIMS technology at Sheffield Hallam University, UK was used. The coating system is equipped with four rectangular unbalanced magnetrons, which can be operated in HIPIMS or standard magnetron sputtering mode.

The coatings were deposited on mirror polished (1 μm diamond paste finish, R_a in the range 15–20 nm) CoCrMo (ASTM F75) alloy coupons and Si (001) wafers. The chemical composition of the medical grade CoCrMo (ASTM F75) alloy is listed in Table 1.

The mirror polished substrates were cleaned in an automated industrial size ultrasonic cleaning line comprising of number of tanks filled with alkaline cleaning water solutions and de-ionised (DI) water for rinsing. Subsequently, the substrates were subjected to surface drying at a high temperature of 95 °C in a vacuum dryer. Prior to the coating deposition, the substrates were subjected to adhesion enhancing ion etching process achieved by bombarding the surface by a mixture of Nb^+ and Ar^+ ions generated by HIPIMS discharge sustained on a Nb target in Ar atmosphere (Ehiasarian et al., 2006). The ion mixture was accelerated towards the substrate by applying a high bias voltage of about −1000 V using a dedicated HIPIMS compatible bias power supply (Ehiasarian et al., 2011). The ion etching of the substrate surface removes the thin native oxide layer and produces a shallow Nb^+ metal ions implanted zone. This ion implanted zone exhibits a well-defined crystalline structure, which promotes the localized epitaxial growth of the coating, resulting in excellent coating to substrate adhesion (Ehiasarian et al., 2007).

The metal ion etching steps is followed by the deposition of thin (~250 nm) base layer of NbN, which provides smooth hardness transition therefore stress transition from the soft CoCrMo substrate to the superhard TiN/NbN top layer resulting in further enhancement of coating adhesion and impact load resistance.

In the final step, TiN/NbN is deposited by sputtering of two opposing pairs of Nb and Ti targets (99.8% pure) in a common $Ar+N_2$ atmosphere at total pressure of 3.4×10^{-1}Pa. In this process a mixed sputtering mode was used by operating one magnetron from each pair in HIPIMS and the other in UBM regime. The coated samples were mounted on a special turn table allowing three-fold rotation. No special shielding was used to guide or restrict the plasma streams originating from the sputtered target surfaces, which provides for high deposition rate. In such coating geometry the multilayering is achieved due to the sequential exposure of the coated surface to the incoming sputtered material fluxes from the magnetrons. TiN/NbN coatings were deposited at temperature of 400 °C maintained in the process by computer controlled external heaters.

2.2. Coating characterisation techniques

The coatings were characterised using various analytical techniques:

- Coating phase composition and texture analyses were carried out by high angle XRD using Malvern PANanalytical Empyrean, Malvern, UK diffractometer with Co source, whereas low angle XRD was employed to define the superlattice period, Δ (bilayer thickness) of the coating.
- FEI Nova-NanoSEM 200 scanning electron microscope was used to image microstructure and surface morphology of the coatings.
- The hardness and Young's modulus were measured in a nano indentation tester (CSM Instruments SA) using Berkovich indenter. The nano hardness value, Hp was calculated using the Oliver-Pharr

Table 1
Chemical composition of CoCrMo alloy (F75).

Element	Cr	Mo	Ni	C	Si	Mn	S	N	Co
wt.%	27–30	5–7	≤0.5	≤0.35	≤1.0	≤1.0	≤0.10	≤0.25	Balance

method under an applied normal a load of 10 mN. This value was averaged after producing 20 indentations. The same instrument was used to produce the loading and unloading curves for different indentation loads in the range of 10 mN–300 mN.

- Coating behaviour (crack formation) under a concentrated load applied by nanoindentation was investigated by focused ion beam cross-sections (FIB) using the FEI Helios Nanolab G3 with a Ga^+ ion source operated at 30 kV instrument.
- Cross-sectional transmission electron microscopy (XTEM) was employed to image the nanoscale multilayer coating architecture. The FIB sections were examined using a cold field emission gun (c-FEG) JEOL F200 TEM.

3. Results and discussion

3.1. Coatings phase composition and texture

An Empyrean X-ray diffractometer (Malvern PANalyitcal Empyrean) with Co source was used to reveal the coating's phase composition, the texture coefficient and calculate the superlattice period of the TiN/NbN multilayer coating.

The high-angle Brag-Brentano (BB) geometry (35°–120°) with a scan rate of 0.013° per second) XRD pattern of the coating (Fig. 1a), showed that only one diffraction pattern exists, which is equivalent to fcc NaCl unit-cell structure with diffraction peaks situated between the positions of CrN and NbN, therefore corresponding to positions of the weighted average of the constituent layers. The high intensity peak centred at 2θ = 48.14° was assigned to (200), indicating most of the grains are oriented along (200). This was further confirmed by the calculated T* (texture) parameter values shown in Table 2. The other low intensity peaks at 41.39°, 85.36°, 89.90° and 110.52° were assigned to (111), (311), (222) and (400) respectively.

Texture parameter, (T*) was calculated using the following equation:

$$T^* = \frac{I_{hkl}/R_{hkl}}{(1/n)\sum_0^n (I_{hkl}/R_{hkl})}$$

where $I_{(hkl)}$ is the measured peak intensity from the (hkl) reflections, R_{hkl} is the reference standard (random) peak intensity from the (hkl) reflections and n is the number of reflections considered (Rickerby et al., 1989; Lewis et al., 1999). The ICDD values of peak intensity were used as the standard reference (R_{hkl}) intensity values since it was not possible to determine R_{hkl} intensity values for a randomly oriented coating material.

Table 2
Texture parameter.

Material	T* (%)				
	{111}	{200}	{311}	{222}	{400}
TiN/NbN multilayer coating	0.47	46.59	0.52	20.63	31.79

3.2. Determination of superlattice period (Δ)

Fig. 2 shows the low-angle diffraction pattern taken in BB (θ-2θ) geometry with an angular step size of 0.003° between 2θ values of 2° and 10°. A very sharp first order peak at 3.38° was observed along with traces of second and third order peaks at 4.3° and 6.58° respectively. This observation of the higher order peaks indicated the formation of more pronounced superlattice structure with minimal intermixing of the two material (TiN and NbN) systems. The sharp peak at 3.38° (first order reflection) was considered for calculating the superlattice period Δ using the standard Bragg equation (Lewis et al., 1999):

$$\Delta = \frac{n\lambda}{2\ \sin\theta}$$

where θ is the Bragg angle, λ is wavelength of incident ray and n is the order of reflection. The calculated superlattice period was Δ = 3.0 nm.

3.3. Microstructure analysis by scanning electron microscopy (SEM)

Fig. 3a shows the cross-section SEM images of TiN/NbN superlattice coatings deposited on silicon wafers. Owing to the high ion bombardment and therefore high adatom mobility during coating growth due to

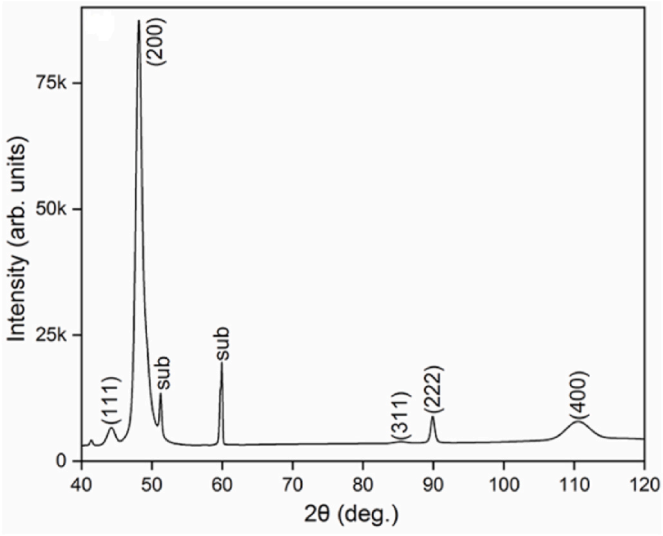

Fig. 1. High-angle XRD diffraction patterns of TiN/NbN multilayer coating.

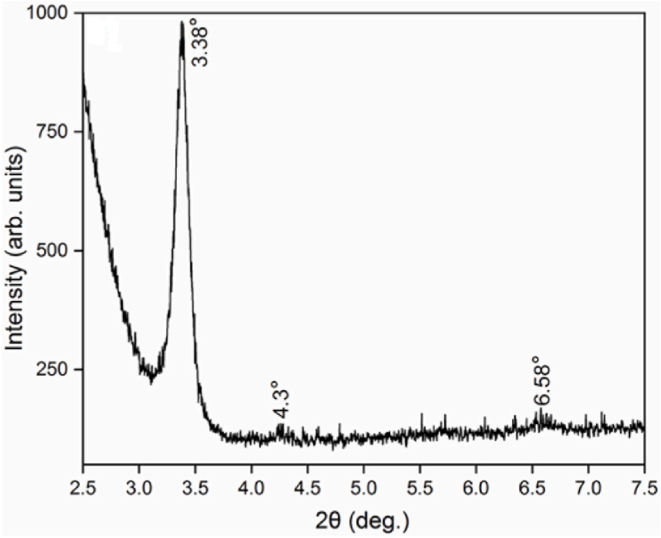

Fig. 2. Low-angle XRD diffraction patterns of TiN/NbN multilayer coating.

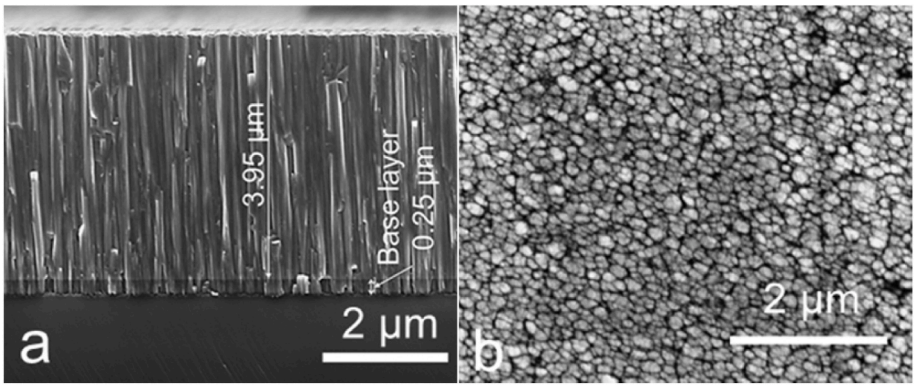

Fig. 3. SEM images of TiN/NbN multilayer coating a) Cross-section (Si substrate); b) Plan view (polished CoCrMo alloy substrate).

the utilisation of HIPIMS, the coating exhibited an extremely dense, void free columnar structure. The individual columns are wide and terminated with smooth column tops which are in stark contrast to coatings deposited under low ion irradiation conditions typically observed when low ionisation techniques such as UBM for example are employed. In such cases, the low adatom mobility results in the formation of rough dome shaped columns and under-dense structure. The micrograph also depicts the 0.25 µm thick and importantly very dense NbN base layer above the coating-substrate interface. The NbN base layer not only provides smooth transition in hardness between the base material and the superhard topcoat but owing to the high nobility of Nb acts as a barrier against substrate corrosion, which is essential in implant applications.

Fig. 3b shows the surface morphology of TiN/NbN coatings deposited on CoCrMo substrates. The surface morphology of the coatings further confirmed that the column tops are indeed smooth, which contributes to the small value for the surface roughness of $R_a = 0.06$ µm. In comparison the surface roughness of state-of-the-art arc deposited monolithically grown TiNbN is at least one order of magnitude higher due to the large amount of droplet phase (Anders, 2008) landing on the surface during coating growth and therefore producing great deal of surface defects, which are detrimental for the corrosion performance of the coatings for implant applications (Hovsepian et al., 2016).

3.4. Microstructure analysis of the as deposited coating by transmission electron microscopy (TEM)

Cross sectional TEM analyses were carried out to reveal the nanolayered structure of the TiN/NbN superlattice coatings. The superlattice structure of the coating consisting of repeating TiN and NbN layers can be seen from the Frensel contrast, Fig. 4. The XTEM image was used to define the bi-layer thickness of $\Delta = 3.0$ nm by direct measurement, which corresponded to the value calculated from the low angle XRD pattern. The image depicts a region where two adjacent columns (labelled in the picture as column A and B) are clearly visible, showing that the overall crystal structure is columnar. This is typical for the PVD grown thin films where the initial stages of the condensation process are dominated by island growth. The layered structure on nanoscale inside of the columns, which is formed due to the repeated sequential deposition of TiN and NbN as explained in section 2.1 is also clearly resolved. The individual layers appear with different contrast due to the atomic weight difference between Ti and Nb. The layers are slightly curved in the coating growth direction due to the interplay between the atomic shadowing effect and the presence of surface tension during the growth process. When the deposition takes place on a flat surface the layers appear laterally forming a 90-degree angle with the growth direction. One of the important messages from this micrograph however, is the extremely dense, void free intercolumnar structure, which is a fingerprint of the HIPIMS process utilising highly ionised plasma flux for the thin film growth. The high energy of the arriving condensing species results in high ad-atom mobility, which allows them to effectively bridge the gaps between the individual columns during the coating growth and densify the coating structures. In contrast, large voids produced with high density are formed when the ionisation levels of the sputtered atoms are low as it is in the case of the standard DC magnetron sputtering. A bright field TEM image of such coating is shown in Fig. 4b for

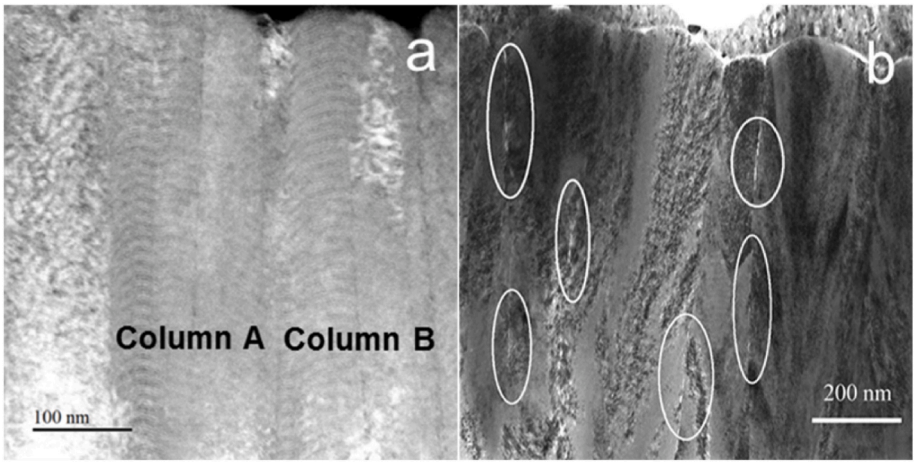

Fig. 4. Cross section TEM images of: a) TiN/NbN deposited by HIPIMS and b) CrN/NbN, deposited by standard unbalanced magnetron sputtering (Hovsepian et al., 2016).

comparison.

3.5. TiN/NbN superlattice coating load bearing capacity and crack formation mechanism

The hardness and elastic modulus of TiN/NbN when deposited on CoCrMo substrate were defined by nanoindentation using Berkovich indenter. During the measurements, the load was increased up to a maximum value of 20 mN at the rate of 40 mN per min and then decreased at the same rate to zero. The indentation depth was monitored to be less than 1/10th of the coating thickness to avoid the influence of the substrate on the hardness measurements. TiN/NbN multilayer coating exhibited high nano hardness and elastic modulus value of Hp = 28 GPa and E = 390 GPa respectively. Similar procedure was followed to determine the hardness and the elastic modulus of the bare CoCrMo alloy, which were found to be as low as Hp = 6 GPa and E = 215 GPa. For the relatively high elastic modulus ratio of the current hard film/soft substrate combination in the range of $E_{coating}/E_{substrate} = 1.81$ indicating that the substrate does not provide the necessary load bearing support for the brittle thin film, and so the fracture toughness of the coating becomes one of the lifetime defining properties for the coating. However, despite of the relatively high elastic moduli ratio our previous research showed that TiN/NbN-CoCrMo system has surprisingly high impact load resistance and high fracture toughness, which was attributed to the high coating integrity and exceptionally strong coating-substrate adhesion bonding (Sugumaran et al., 2021). In the current investigation, the emphasis was put on the more detailed understanding on the role of the coating architecture behind the enhanced fracture toughness of the superlattice TiN/NbN films when deposited on medical grade CoMoCr alloys.

The fracture toughness and crack initiation mechanism in TiN/NbN superalattice structured coatings deposited on CoCrMo alloy substrate was investigated by nanoindentation using Berkovich indenter by applying a concentrated normal load in wide range between 10 mN and 300 mN. The method has been successfully used to develop 3D Finite Element models for stress evolution for systems with wide range variation of the $E_{coating}/E_{substrate}$ = between 2.33 and 41.86 (Fu et al., 2015). Fig. 5 a, b and c depicts the pyramidal impressions produced on the surface of the coating under various applied indentation loads. In this experiment no cracks were observed to form at the corners of the indent, which is clear example for the high fracture toughness of the superlattice structured coatings. The result confirms the observations from our previous experiments with Vickers indentations using several orders of magnitude higher indentation loads of 30 kgf where no radial crack formation along the edges of the indent were found (Sugumaran et al., 2021).

The employment of nanoindentation technique using smaller loads in the mN range in this study however, allows for a very precise monitoring of the conditions for crack development by studying the material behaviour during loading and unloading. Fig. 6 a, b and C shows the load-indenter displacement curves during loading and unloading for maximum applied load of 10 mN, 100 mN and 300 mN respectively.

The loading curves for the smaller 10 mN and 100 mN loads were very smooth without any sudden changes. However, the loading curve at 300 mN peak load shows a clear kink when the normal load reaches values of about 200 mN, which is a sign of that a certain sudden event taking place in the coating material at this point. We assume that the sudden event is a crack initiation event. A similar change in the loading curve but at a smaller scale is observed at higher load of around 260 mN before reaching the maximum preselected indentation load of 300 mN which is a fingerprint of dynamic processes. The arrows in Fig. 6c indicate kinks in the loading curve due to such sudden events. The unloading curves for all the three different loads were smooth, which shows that the sudden events in the coating material occur dynamically only during loading when the exerted mechanical pressure is gradually increasing.

Post indentation cross sectional FIB SEM and TEM analyses were carried out to investigate the structure of the deformed coating material under the indenter for the case of 300 mN applied load. The material in the indent was sectioned along one of the diagonals of the three spike Berkovich indentation, as shown in Fig. 5 using FIB-SEM technique. Low magnification of the FIB section is shown in Fig. 7 where the bright contrast horizontal line in the middle of the image represents the coating and the substrate interface. Two symmetrical cracks appearing as bright contrast curved lines can be seen originated from the interface and propagating into the coating material.

The high magnification TEM image shown in Fig. 8 reveals further important details in the crack formation and propagation mechanism during coating indentation.

The indentation crater on the top of the coating is clearly visibible to a depth of 950 nm. The image shows the dense void free columnar structure where the columns are terminated with dome shaped tops to create a very smooth surface as already discussed in 3.2. While the columns outside of the indentation volume are wider and strictly vertical, following the coating growth direction (Zone B), the columns directly under the indentor tip, (Zone A) appear more squashed (plastically deformed) and rotated to form a V-shaped (in the plane of the cross section) volume, the boundaries of which are schematically indicated by white lines (Fig. 8). The columns beneath this zone however, appear to have retained their width and vertical direction. The darker contrast ribbon at the coating/substrate interface at the bottom of the cross section is the 250 nm thick NbN base layer. The XTEM image also reveals that the substrate beneath the indented volume of the coating has yielded and sunked to form a 250 nm deep step with the non deformed original substrate surface. Clearly, in this transition volume the principal stress changes its direction and level. It has been reported that the stiffness between plastic zone and elastic material surrounding may cause large tensile stress outside the impression (Fu et al., 2015). In systems such superhard TiN/NbN coating deposited on relatively soft substrate such as CoCrMo alloy where the elastic modulus ratio is large,

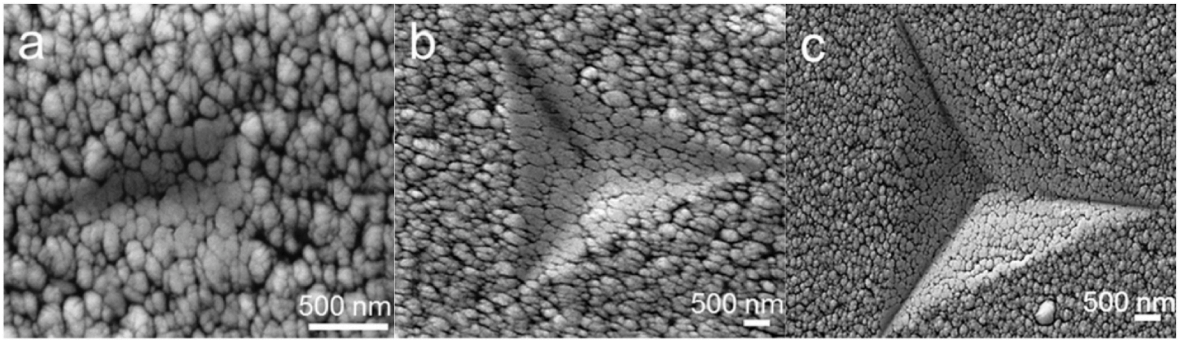

Fig. 5. SEM images of the Berkovich indentations under various applied loads: a) 10 mN, b) 100 mN and c) 300 mN.

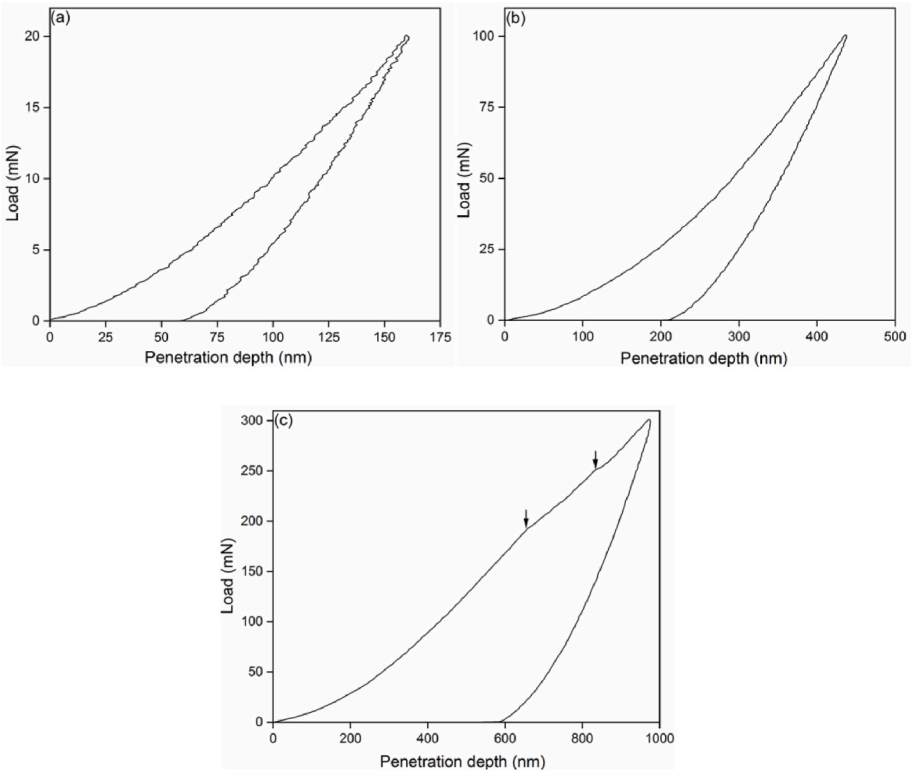

Fig. 6. Load indentation depth curves for a peak load of: a) 10 mN, b) 100 mN and c) 300 mN.

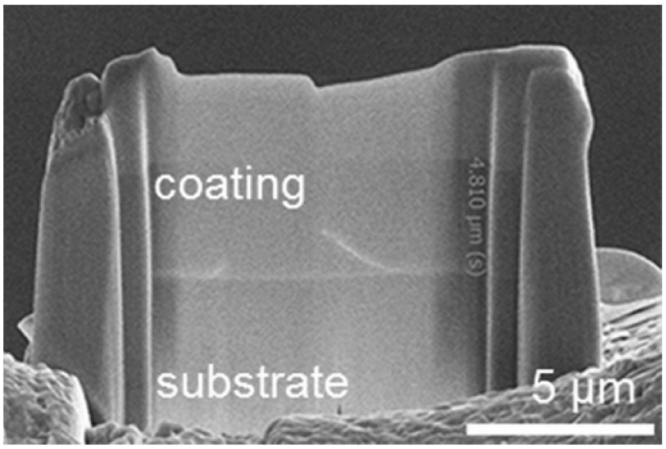

Fig. 7. FIB cross section SEM image of the deformed coating material in the indentation crater.

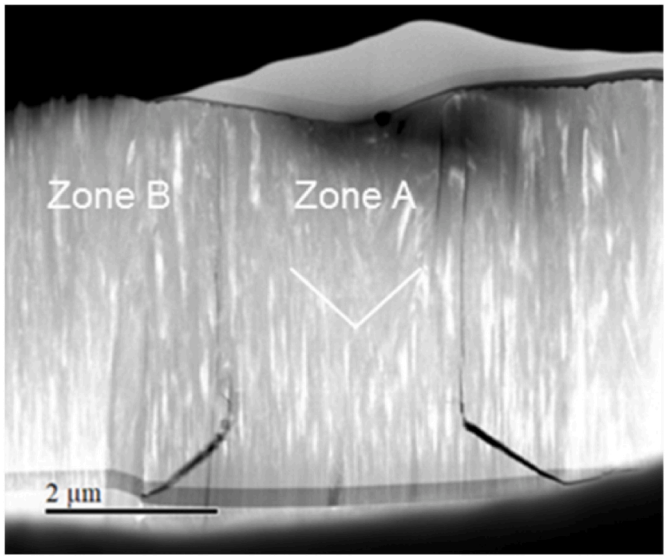

Fig. 8. Cross section TEM immage of the indented TiN/NbN coating.

the tensile stress at the edge of the impression can reach high enough levels for crack initiation. As it can be seen in Fig. 8, the cracks initiated in the weaker substrate material propagate into the coating initially at approximately 45° to up to 800 nm distance from the interface and then propagate vertically to reach the coating surface. Apparently the direction for crack propagation is defined by the crystallographic orientation/texture of the coating material. The material will plastically deform by slip events taking place at the crystallographic planes with the most favourable orientation and with the highest atomic population. Hence, initially the cracks will follow the orientation of such slip planes and thereafter will propagate through the vertical intercolumnar boundaries where the atomic bonding is weaker.

Another important observation is that despite of the sizeable plastic deformation of the substrate material under the indentation, the NbN base layer/substrate bonding has remained uncompromised. Due to the application of the HIPIMS surface pre-treatment, as described in section 2.1, no lateral cracks or delamination were observed to form in this critical zone in the coating, which demonstrates the strong coating adhesion as previously reported based on scratch test results (Sugumaran et al., 2021).

Further details of the material response to the applied concentrated indentation load and the behaviour of the layered on nanoscale structure in particular are provided by the higher magnification XTEM image in Fig. 9. Part of the indentation crater which is directly under the indenter tip is clearly visible at the top left hand corner of the image. As already

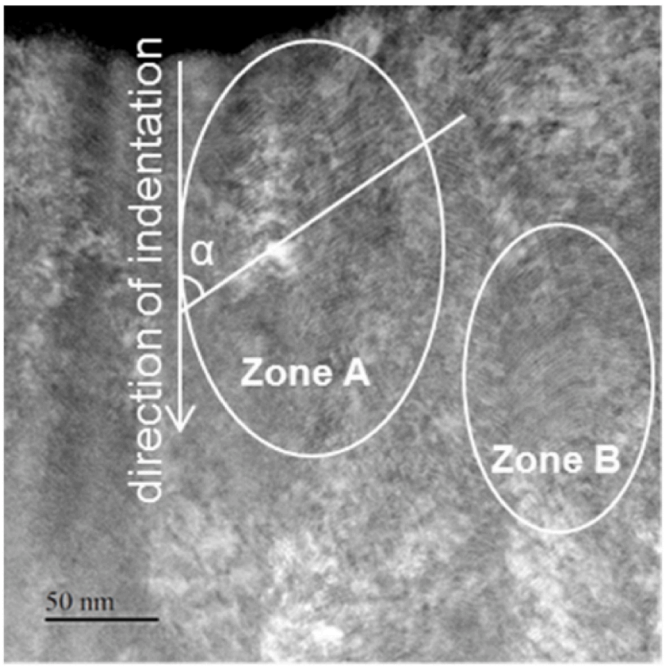

Fig. 9. Higher magnification XTEM image of TiN/NbN superlattice coating after 300 mN Berkovich indentation.

described with Fig. 4a the general columnar structure with well defined nanolayers inside of each column is also well resolved. However, there is a stark difference in the layer appearance between the layers in the coating zone directly under the indentation crater (highlighted as zone A) and the layers which are far from the crater (highlighted as zone B) in Fig. 9. The layers in zone B are curved with a certain waviness, which is typical for the as deposited non deformed superlattice structured coatings as already discussed in 2.1. The layers in Zone A however, appear straight and aligned, following the indentation crater shape. Clearly the layer directionality and shape results from the substantial plastic deformation that the coating material experiences during the indenter penetration. The image shows that the individual layers in Zone A appear to be rotated at an specific angle **α** but importantly the well ordered multilayer structure with sharp interfaces is well preserved.

It has been previously reported that in monolythically grown PVD coatings the individual columns can be plastically deformed and bent under application of tangential, load (in the reported example exerted by frictional force) (M ü nz et al., 2001; Zhou et al., 2010). In such coatings however, the column deformation and bending opens intercolumnar cracks, which significantly compromise coating integrity and therefore performance. Such collective alignment and rotation of large number of individual layers, due to applied mechanical indentation load inducing plastic deformation of the material but still maintaining their general multilayer order is observed for the first time for superlattice structured coatings. The ability of the layered structures to adapt to the load/deformation conditions at the same time preserving their peculiar structural characteristics without major failure is undisputably a sign for an exeptionally high toughness, which is a great advantage of the layered materials at the nanoscale as compared to monolithically grown coatings.

It is important to comment that the synergy between the enhanced fracture toughness of the layered materials on the nanoscale and the high coating substrate-adhesion achieved through the use of the HIPIMS etching process which induces metal ion implantation and a specially engineered interface (Ehiasarian et al., 2006, 2007) results in significant reduction of the fatigue deficit of the base material in contrast to the higher fatigue deficits encountered when a brittle thin film is deposited on a ductile substrate. Fine research results have described this phenomenon in such systems, which occurs under load due to the initiation of cracks in the brittle coating which penetrate into the substrate resulting in premature failure (Guo et al., 2015, 2018; Bai et al., 2021). In all cases described in this literature however, there is clear evidence for poor coating-substrate adhesion substantiated by the observed coating debonding. In contrast when HIPIMS surface pretreatment is combined with deposition of a superlattice-structured coating we have consistently observed a reduction of the fatigue deficit (Braun et al., 2010) and even an increase of the fatigue strength; examples include CrN/NbN coatings on medical implants (Hovsepian et al., 2016) and on steam turbine blades (Hovsepian et al., 2018).

The current paper sheds further light on the reasons for the exceptionally high toughness of the nanoscale multilayer/superallatice coatings. We have observed for the first time that during indentation a collective rotation and alignment of the individual layers of the superlattice stack takes place without compromising coating integrity. It was further found that in such a material combination (superhard coating deposited on ductile substrate, $E_{coating}/E_{substrate} = 1.81$), cracks will initiate underneath the coating due to substrate deformation and then propagate towards the coating surface.

4. Conclusions

- Superlattice TiN/NbN coatings with superlattice period of $\Delta = 3.0$ nm exhibiting f.c.c. crystallographic structure with {200} preferred orientation have been successfully deposited on medical grade CoCrMo alloy substrate by mixed HIPIMS-UBM process.
- In the case of TiN/NbN deposited on CoCrMo alloy the relatively high $E_{coating}/E_{substrate} = 1.81$ indicates that the substrate does not provide the necessary load bearing support for the brittle thin film, the utilisation of Berkovich indentation technique proved to be a potent approach to study coating material as well as structural response to applied concentrated load.
- FIB/SEM analyses of the indented coatings revealed that in the hard-on-soft material systems the cracks will initiate due to sub-coating substrate deformation and then propagate towards the coating surface. The cracks initiate at the rim of the plastically deformed substrate zone where the principal stress changes its direction and level to cause large tensile stress.
- The FIB/SEM and low magnification XTEM analysis showed that an exceptionally strong coating substrate adhesion bonding was achieved due to the utilisation of the HIPIMS pre-treatment as no coating delamination was observed to take place due to the indentation test.
- High resolution XTEM analyses showed that during the indentation a collective rotation and alignment of the individual layers of the superlattice stack takes place. The ability of the layered structures to adapt to the load/deformation conditions preserving their peculiar structural characteristics at the same time without major failure, is undisputably a clear evidence for an exceptionally high toughness, which is a great advantage of the layered materials at the nanoscale as compared to monolithically grown coatings.
- The high toughness of the superlattice structured TiN/NbN coatings combined with their exceptionally high adhesion on madical grade CoCrMo alloys as well as reliable barrier properties as previously reported categorises them as a strong candidate for medical implant applications.

CRediT authorship contribution statement

Papken Ehiasar Hovsepian: Writing – original draft, Methodology. **Arunprabhu Arunachalam Sugumaran:** Investigation, Formal analysis. **Mark Rainforth:** Writing – review & editing. **Jiahui Qi:** Formal analysis. **Imran Khan:** Validation. **Arutiun Papken Ehiasarian:** Writing – original draft, Methodology.

Declaration of competing interest

The authors declare that they have no known competing financial interests or personal relationships that could have appeared to influence the work reported in this paper.

References

Anders, A., 2008. Some Applications of Cathodic Arc Coatings.

Bai, Y., Guo, T., Wang, J., Gao, J., Gao, K., Pang, X., 2021. Stress-sensitive fatigue crack initiation mechanisms of coated titanium alloy. Acta Mater. 217 https://doi.org/10.1016/j.actamat.2021.117179.

Blunn, G.W., Ferro De Godoy, R., Meswania, J., Briggs, T.W.R., Tyler, P., Hargunani, R., et al., 2019. A novel ceramic coating for reduced metal ion release in metal-on-metal hip surgery. J. Biomed. Mater. Res. B Appl. Biomater. 107.

Blunt, L., Bills, P., Jiang, X., Hardaker, C., Chakrabarty, G., 2009. The role of tribology and metrology in the latest development of bio-materials. Wear 266.

Braun, R., Schulz, U., Leyens, C., Hovsepian, P.E., Ehiasarian, A.P., 2010. Oxidation and fatigue behaviour of γ-TiAl coated with HIPIMS CrAlYN/CrN nanoscale multilayer coatings and EB-PVD thermal barrier coatings. Int. J. Mater. Res. 101 https://doi.org/10.3139/146.110323.

Chen, Y., Guo, T., Wang, J., Pang, X., Qiao, L., 2021. Effects of orientation on microstructure and mechanical properties of TiN/AlN superlattice films. Scripta Mater. 201 https://doi.org/10.1016/j.scriptamat.2021.113951.

Ehiasarian, A.P., 2007. Fundamentals and applications of HIPIMS. In: Wei, R. (Ed.), Plasma Surf Eng Res its Pract Appl. First. Kerala, vol. 4. Research Signpost, India.

Ehiasarian, A., Hovsepian, P., Munz, W., 2006. Combined coating process comprising magnetic field-assisted, high power, pulsed cathode sputtering and an unbalanced magnetron. US Pat 7,81,1862. https://www.google.com/patents/US70811863.

Ehiasarian, A.P., Wen, J.G., Petrov, I., 2007. Interface microstructure engineering by high power impulse magnetron sputtering for the enhancement of adhesion. J. Appl. Phys. 101.

Ehiasarian, A.P., Tietema, R., Bugyi, R., Klimczak, A., Eh, P., Hovsepian, D.D., 2011. A Vacuum Treatment Apparatus, a Bias Power Supply and a Method of Operating a Vacuum Treatment Apparatus. United States.

Fu, K., Chang, L., Zheng, B., Tang, Y., Yin, Y., 2015. Analysis on cracking in hard thin films on a soft substrate under Berkovich indentation. Vacuum 112.

Guo, T., Qiao, L., Pang, X., Volinsky, A.A., 2015. Brittle film-induced cracking of ductile substrates. Acta Mater. 99 https://doi.org/10.1016/j.actamat.2015.07.059.

Guo, T., Chen, Y., Cao, R., Pang, X., He, J., Qiao, L., 2018. Cleavage cracking of ductile-metal substrates induced by brittle coating fracture. Acta Mater. 152 https://doi.org/10.1016/j.actamat.2018.04.017.

Hoseini, M., Jedenmalm, A., Boldizar, A., 2008. Tribological investigation of coatings for artificial joints. Wear 264.

Hovsepian, P.E., Münz, W.D., 2002. Recent progress in large-scale production of nanoscale multilayer/superlattice hard coatings. Vacuum.

Hovsepian, P.E., Lewis, D.B., Münz, W.D., 2000. Recent progress in large scale manufacturing of multilayer/superlattice hard coatings. Surf. Coating. Technol. 9, 133–134.

Hovsepian, P.E., Münz, W.-D., 2006. Synthesis, structure, and applications of nanoscale multilayer/superlattice structured PVD coatings. In: Cavaleiro, A., De Hosson, J.T.M. (Eds.), Nanostructured Coatings [Internet]. Springer New York, New York, NY, pp. 555–644. https://doi.org/10.1007/978-0-387-48756-4_145. Available from:

Hovsepian, P.E., Ehiasarian, A.P., Purandare, Y., Sugumaran, A.A., Marriott, T., Khan, I., 2016. Development of superlattice CrN/NbN coatings for joint replacements deposited by high power impulse magnetron sputtering. J. Mater. Sci. Mater. Med. 27, 147. https://doi.org/10.1007/s10856-016-5751-08.

Hovsepian, P.E., Ehiasarian, A.P., Purandare, Y.P., Mayr, P., Abstoss, K.G., Mosquera Feijoo, M., Schulz, W., Kranzmann, A., Lasanta, M.I., Trujillo, J.P., 2018. Novel HIPIMS deposited nanostructured CrN/NbN coatings for environmental protection of steam turbine components. J. Alloys Compd. 746 https://doi.org/10.1016/j.jallcom.2018.02.312.

Łapaj, Ł., Markuszewski, J., Wendland, J., Mróz, A., Wierusz-Kozłowska, M., 2016. Massive failure of TiNbN coating in surface engineered metal-on-metal hip arthroplasty: retrieval analysis. J. Biomed. Mater. Res. B Appl. Biomater. 104.

Lewis, D.B., Donohue, L.A., Lembke, M., Münz, W.D., Kuzel, R., Valvoda, V., et al., 1999. The influence of the yttrium content on the structure and properties of Ti1-x-y-zAlxCryYzN PVD hard coatings. Surf. Coating. Technol. 114.

Münz, W.D., Lewis, D.B., Hovsepian, P.E., Schönjahn, C., Ehiasarian, A., Smith, I.J., 2001. Industrial scale manufactured superlattice hard PVD coatings. Surf. Eng. 17, 15–27.

McGregor, D.B., Baan, R.A., Partensky, C., Rice, J.M., Wilbourn, J.D., 2000. Evaluation of the carcinogenic risks to humans associated with surgical implants and other foreign bodies - a report of an IARC Monographs Programme Meeting. Eur. J. Cancer.

Okazaki, Y., Gotoh, E., 2005. Comparison of Metal Release from Various Metallic Biomaterials in Vitro. Biomaterials.

Rickerby, D.S., Jones, A.M., Bellamy, B.A., 1989. X-ray diffraction studies of physically vapour-deposited coatings. Surf. Coating. Technol. 37.

Serro, A.P., Completo, C., Colaço, R., dos Santos, F., da Silva, C.L., Cabral, J.M.S., et al., 2009. A comparative study of titanium nitrides, TiN, TiNbN and TiCN, as coatings for biomedical applications. Surf. Coating. Technol. 203.

Sugumaran, A.A., Purandare, Y., Shukla, K., Khan, I., Ehiasarian, A., Hovsepian, P., 2021. TiN/NbN nanoscale multilayer coatings deposited by high power impulse magnetron sputtering to protect medical-grade CoCrMo alloys. Coatings 11.

Wapner, K.L., 1991. Implications of metallic corrosion in total knee arthroplasty. Clin. Orthop. Relat. Res.

Yang, S., Camino, D., Jones, A.H.S., Teer, D.G., 2000. Deposition and tribological behaviour of sputtered carbon hard coatings. Surf. Coating. Technol. 124.

Zhou, Z., Rainforth, W.M., Luo, Q., Hovsepian, P.E., Ojeda, J.J., Romero-Gonzalez, M.E., 2010. Wear and friction of TiAlN/VN coatings against Al2O3 in air at room and elevated temperatures. Acta Mater. 58.